THE JOURNAL OF BIOLOGICAL CHEMISTRY VOL. 283, NO. 15, pp. 9543–9554, April 11, 2008

Metabolic Basis of Visual Cycle Inhibition by Retinoid and Nonretinoid Compounds in the Vertebrate Retina*

Received for publication, November 1, 2007, and in revised form, December 20, 2007 Published, JBC Papers in Press, January 14, 2008, DOI 10.1074/jbc.M708982200

Marcin Golczak[‡], Akiko Maeda[‡], Grzegorz Bereta[‡], Tadao Maeda[‡], Philip D. Kiser[‡1], Silke Hunzelmann[‡§], Johannes von Lintig[§], William S. Blaner[¶], and Krzysztof Palczewski[‡2]

From the [‡]Department of Pharmacology, School of Medicine, Case Western Reserve University, Cleveland, Ohio 44106, the [§]Institute of Biology I, Animal Physiology and Neurobiology, Hauptstrasse 1, D-79104 Freiburg, Germany, and the [¶]Department of Medicine, College of Physicians and Surgeons, Columbia University, New York, New York 10032

In vertebrate retinal photoreceptors, the absorption of light by rhodopsin leads to photoisomerization of 11-*cis*-retinal to its all-*trans* isomer. To sustain vision, a metabolic system evolved that recycles all-*trans*-retinal back to 11-*cis*-retinal. The importance of this visual (retinoid) cycle is underscored by the fact that mutations in genes encoding visual cycle components induce a wide spectrum of diseases characterized by abnormal levels of specific retinoid cycle intermediates. In addition, intense illumination can produce retinoid cycle by-products that are toxic to the retina. Thus, inhibition of the retinoid cycle has therapeutic potential in physiological and pathological states. Four classes of inhibitors that include retinoid and nonretinoid compounds have been identified. We investigated the modes of action of these inhibitors by using purified visual cycle components and *in vivo* systems. We report that retinylamine was the most potent and specific inhibitor of the retinoid cycle among the tested compounds and that it targets the retinoid isomerase, RPE65. Hydrophobic primary amines like farnesylamine also showed inhibitory potency but a short duration of action, probably due to rapid metabolism. These compounds also are reactive nucleophiles with potentially high cellular toxicity. We also evaluated the role of a specific protein-mediated mechanism on retinoid cycle inhibitor uptake by the eye. Our results show that retinylamine is transported to and taken up by the eye by retinol-binding protein-independent and retinoic acid-responsive gene product 6-independent mechanisms. Finally, we provide evidence for a crucial role of lecithin: retinol acyltransferase activity in mediating tissue specific absorption and long lasting therapeutic effects of retinoid-based visual cycle inhibitors.

In vertebrate photoreceptor cells, absorbance of light by the visual chromophore, 11-*cis*-retinal, coupled to rhodopsin leads to its photoisomerization to all-*trans*-retinal and initiation of the phototransduction signal cascade (reviewed in Ref. 1). To ensure constant vision, 11-*cis*-retinal is efficiently regenerated by a complex sequence of enzymatic reactions called the visual or retinoid cycle (reviewed in Refs. 2–4). This pathway is located in both retinal pigment epithelium (RPE)[3] and photoreceptor cells. The key enzymatic step of visual chromophore regeneration is the isomerization of all-*trans*-retinyl palmitate and other esters to 11-*cis*-retinol in a reaction catalyzed by RPE65 (5–7).

The importance of the retinoid cycle for maintaining vision is documented by the number and variety of diseases caused by mutations in genes encoding proteins involved in this process (2). Three main strategies have been developed to treat these diseases. The first uses virally mediated transfer gene technology to replace the defective gene. This approach has successfully rescued vision in mouse and dog models of Leber congenital amaurosis and retinitis pigmentosa (8–13). The second approach involving pharmacological supplementation with the missing chromophore primarily applies to diseases characterized by deficits in retinoid biosynthesis (13–16). The third strategy is to attenuate flux of retinoids in the eye by inhibiting specific steps in the retinoid cycle (17–20). This approach is used for diseases associated with accumulation of toxic visual cycle by-products (*e.g.* lipofuscin fluorophores, such as *N*-retinidene-*N*-retinyl ethanolamine (A2E) and its derivatives) that can cause multiple forms of retinal degeneration (21–23). Examples of diseases sharing this phenotype include age-related macular degeneration, retinitis pigmentosa, and Stargardt disease (reviewed in Ref. 2).

Visual cycle inhibitors can be classified into four distinct groups based on their chemical structures. The first consists of 13-*cis*-retinoic acid (13-*cis*-RA) and the hydroxyphenyl amide of its all-*trans* isomer, fenretinide (Fig. 1*A*). These retinoid inhibitors have been used for decades in the treatment of acne and chemoprevention of cancer (24). Clinical reports showing delayed dark adaptation and night blindness upon 13-*cis*-RA

* This work was supported by National Institutes of Health Grants EY09339 and P30 EY11373. The University of Washington licensed some of the technology described here to Acucela Inc. K. P. is a consultant for Acucela Inc. The costs of publication of this article were defrayed in part by the payment of page charges. This article must therefore be hereby marked "*advertisement*" in accordance with 18 U.S.C. Section 1734 solely to indicate this fact.

[1] Supported by the Visual Science Training Program Grant 2T32EY007157 from the NEI, National Institutes of Health.

[2] To whom correspondence should be addressed: Dept. of Pharmacology, School of Medicine, Case Western Reserve University, Wood Bldg., 10900 Euclid Ave., Cleveland, OH 44106-4965. E-mail: kxp65@case.edu.

[3] The abbreviations used are: RPE, retinal pigment epithelium; A2E, *N*-retinidene-*N*-retinyl ethanolamine; CHAPS, 3-[(3-cholamidopropyl)dimethylammonio]-1-propanesulfonate; DMF, *N*,*N*-dimethylformamide; GM, growth medium; LRAT, lecithin:retinol acyltransferase; RA, retinoic acid; RBP, serum retinol-binding protein; Ret-NH_2, all-*trans*-retinylamine; RDH, retinol dehydrogenase; ROS, rod outer segments; TDH, (2*E*,6*E*)-*N*-hexadecyl-3,7,11-trimethyldodeca-2,6,10-trienamine; TDT, (12*E*,16*E*)-13,17,21-trimethyldocosa-12,16,20-trien-11-one; WT, wild type; HPLC, high performance liquid chromatography; MES, 4-morpholineethanesulfonic acid; bis-tris, 2-[bis(2-hydroxyethyl)amino]-2-(hydroxymethyl)propane-1,3-diol; ERG, electroretinogram.

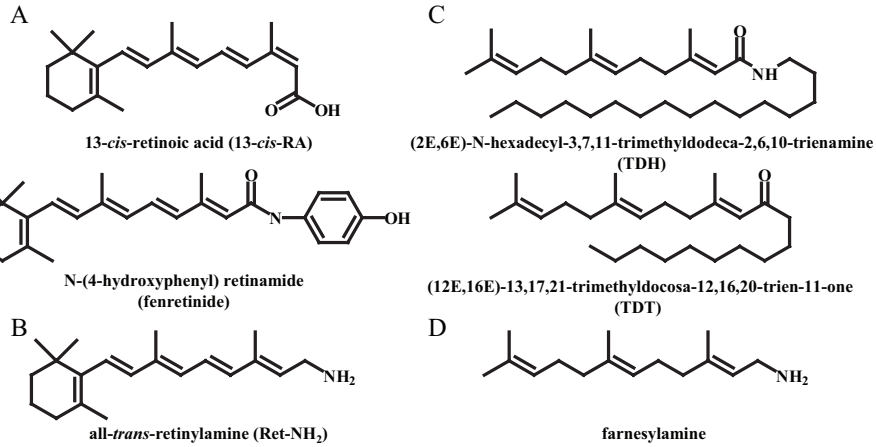

FIGURE 1. **Structures of visual cycle inhibitors and isoprenoids.** Based on their chemical structures, the studied compounds are classified into four groups: retinoic acid derivatives (*A*), positively charged retinoids (*B*), farnesyl-containing isoprenoids (*C*), and nonretinoid hydrophobic primary amines like farnesylamine (*D*).

treatment drew attention to these compounds as potential visual therapeutics (25, 26). 13-*cis*-RA was found to inhibit 11-*cis*-retinol dehydrogenase, which catalyzes the final enzymatic step in the visual cycle (27), and to bind RPE65 (28). Fenretinide slowed the flux of retinoids into the eyes, most probably by reducing levels of vitamin A bound to serum retinol-binding protein (RBP) (17). Both compounds reduced A2E deposition in the eye (18–20). All-*trans*-retinylamine (Ret-NH$_2$) and its derivatives (Fig. 1*B*) may exert similar effects. Developed as a transition state analog for the isomerization reaction, Ret-NH$_2$ inhibits 11-*cis*-retinol production (29, 30). Moreover, Ret-NH$_2$ is reversibly *N*-acetylated by lecithin:retinol acyltransferase (LRAT) and stored in retinosomes within the RPE (30–32). This last characteristic may contribute to its efficient transport and long-lasting inhibition of the retinoid cycle *in vivo*. Farnesyl-containing isoprenoid derivatives, originally characterized by Rando and co-workers (33), belong to the third group of inhibitors. These are thought to act through interaction with RPE65 (Fig. 1*C*), although their therapeutic efficiency is retracted (34). The last class of inhibitors is composed of nonretinoid hydrophobic primary amine with therapeutic potential. These compounds have yet to be evaluated (Fig. 1*D*).

In the present work, we used biochemical, cell culture, and *in vivo* experimental approaches to compare the properties and therapeutic potential of various retinoid cycle inhibitors that might benefit retinal diseases. We evaluated inhibitory efficacy and potency, molecular targets, and modes of action *in vivo* and *in vitro*. Farnesylamine and farnesol derivatives were used to investigate the role of the amino group in inhibiting the retinoid cycle. Finally, we evaluated the role of serum RBP/STRA6 (retinoic acid-responsive gene product 6) in delivering some of these therapeutic agents to the eyes.

MATERIALS AND METHODS

Animals—*Rbp*$^{-/-}$ mice were previously generated and described (35, 36), and their genotypes were confirmed by published protocols (36). All mice were from a mixed C57Bl/6 × sv129 genetic background. *Lrat*$^{-/-}$ mice were generated and genotyped as described previously (55). *Abca*4$^{-/-}$ mice were generated by standard procedures (Ingenious Targeting, Inc., Rochester, NY). The targeting vector was constructed by replacing exon 1 with the *neo* cassette. *Abca4*$^{-/-}$ mice were maintained in a mixed background of C57BL/6 and 129Sv/Ev, and siblings with Leu residue in position 450 (Leu-450) of RPE65 were used. Genotyping of mice was done by PCR using primers ABCR1 (5′-GCCCAGTGGTCGATCTGTCTAGC-3′) and ABCR2 (5′-CGGACACAAAGGCCGCTAGGACCACG-3′) for wild type (WT) (619 bp) and A0 (5′-CCACAGCACACATCAGCATTTCTCC-3′) and N1 (5′-TGCGAGGCCAGAGGCCACTTGTGTAGC-3′) for targeted deletion (455 bp). PCR products were cloned and sequenced to verify their identity.

Typically, 6-week-old mice were used for these experiments. Mice were maintained continuously in darkness, and all experimental manipulations were performed under dim red light passed through an Eastman Kodak Co. Safelight filter. All animal procedures were approved by Case Western Reserve University and conformed with recommendations of the American Veterinary Medical Association Panel on Euthanasia and the Association of Research for Vision and Ophthalmology. Fresh bovine eyes were obtained from a local slaughterhouse (Mahan's Packing, Bristolville, OH), and RPE microsomes were prepared from bovine eyecups (37).

Materials and Chemical Syntheses—13-*cis*-RA and all-*trans*-RA were purchased from Sigma and fenretinide from Toronto Research Chemicals Inc. (Toronto, Canada). (2*E*,6*E*)-*N*-hexadecyl-3,7,11-trimethyldodeca-2,6,10-trienamine (TDH) and (12*E*,16*E*)-13,17,21-trimethyldocosa-12,16,20-trien-11-one (TDT) were synthesized by Acucela Inc. (Bothell, WA). Ret-NH$_2$ was synthesized as previously described (29, 30). Farnesylamine was prepared by reacting farnesyl bromide with potassium phthalimide (38). Reaction progress was monitored by TLC. The chemical structure of farnesylamine derivatized with *N*,*O*-bis(trimethylsilyl)trifluoroacetamide in the presence of 10% of trimethylchlorosilane was validated by gas chromatography-mass spectrometry.

Stable Transduction of the NIH3T3 Cell Line—An NIH3T3 stable cell line expressing LRAT and two double-stable cell lines expressing LRAT/RPE65 and LRAT/STRA6 were used. Full-length human LRAT, RPE65, and STRA6 clones used to prepare these cell lines were purchased from the American Type Culture Collection (Manassas, VA). For construction of retroviral expression vectors, LRAT, RPE65, and STRA6 cDNA were amplified by PCR, and EcoRI and NotI restriction sites were introduced at the ends of the coding sequence by using the following primers: STRA6, GCAGATGAATTCACCATGTCGTCCCAGCCAGCAGG and CGTCTAGCGGCCGCTCAGGGCTGGGCACCATTGG; LRAT, GAGGTGAATTCAGCTACTCAGGGATGAAGAACCCCATGCTG and ACTGACG-

CGGCCGCATGAAGTTAGCCAGCCATCCATAG; RPE65, TCTGGGAATTCAACTGGAAGAAAATGTCTATCCAGGTTGAG and CTTGCTGGCGGCCGCTCAAGATTTTTTGAACAGTCC. These primers were cloned into the pMXs-IG (STRA6 and RPE65) or pMXs-IP (LRAT) retroviral vectors provided by Dr. T. Kitamura (University of Tokyo) (39). Inserts were sequenced and confirmed to be identical to LRAT, RPE65, and STRA6 reference sequences deposited in the Ensembl data base. The Phoenix-Eco retroviral producer cell line as well as the NIH3T3 cells were cultured in growth medium (GM) consisting of Dulbecco's modified Eagle's medium, pH 7.2, with 4 mM L-glutamine, 4,500 mg/liter glucose, and 110 mg/liter sodium pyruvate, supplemented with 10% heat-inactivated fetal bovine serum, 100 units/ml penicillin, and 100 units/ml streptomycin. Cells were maintained at 37 °C in 5% CO_2. Twenty-four hours prior to transfection, 2.5×10^6 Phoenix-Eco cells were seeded on a 6-cm plate and cultured in 6 ml of GM. To generate a transfection mixture, 1 ml of 50 mM HEPES, pH 7.05, containing 10 mM KCl, 12 mM dextrose, 280 mM NaCl, and 1.5 mM Na_2HPO_4 was added to an equal volume of 250 mM $CaCl_2$ solution containing 20 μg of plasmid DNA, mixed, incubated for 1 min, and added dropwise to the cells. This medium was replaced with fresh GM 8 h after transfection and replaced again 24 h later. The retroviral supernatant was harvested 48 h post-transfection, centrifuged at 1,500 rpm for 5 min to remove detached cells, aliquoted into 0.5-ml portions, frozen in liquid nitrogen, and stored at −80 °C. 24 h prior to transduction, 2×10^5 NIH3T3 fibroblasts were plated per 6-cm dish in 6 ml of GM. For transduction, this medium was replaced with a mixture consisting of 2.5 ml of GM (the one just collected, not fresh GM), 0.5 ml of viral supernatant, and 5 μg/ml Polybrene. The plate was gently swirled and incubated for 24 h at 30 °C in 5% CO_2 before replacing the medium with fresh GM. After reaching confluence, cells were split and seeded at 2×10^5. This infection cycle was repeated 2–4 times.

LRAT, Retinol Dehydrogenase (RDH), and Enzymatic Isomerization Assays—The LRAT activity assay was carried out in 10 mM Tris/HCl buffer, pH 7.5, containing 1% bovine serum albumin (final volume 200 μl). All-*trans*-retinol was delivered in 0.8 μl of *N*,*N*-dimethylformamide (DMF) to a final concentration of 10 μM, and the reaction was initiated by the addition of bovine RPE microsomes (150 μg of protein). Reaction mixtures were incubated at 30 °C for 10 min, stopped by injecting 300 μl of methanol, and mixed with the same volume of hexane. Retinoids were extracted and analyzed on a Hewlett Packard 1100 series HPLC system equipped with a diode array detector and a normal phase column (Agilent-Si; 5 μm, 4.5 × 250 mm) eluted with 10% ethyl acetate in hexane at a flow rate of 1.4 ml/min.

Activities of RDH in bovine rod outer segments (ROS) and RPE microsomes were assayed by monitoring retinol production (reduction of retinal). Each reaction mixture (200 μl) contained 50 mM MES, pH 5.5, 1 mM dithiothreitol, 200 μg of UV-treated RPE microsomes or ROS, the test substrate, and a reducing agent (NADH or NADPH). For RDH5, the reaction was initiated by the addition of 11-*cis*-retinal (2 μM) followed by 60 μM NADH. To detect RDH activity in ROS, NADPH (60 μM) was added first, and the samples were exposed to a single flash of light from an electronic flash (40). Reaction mixtures were incubated at 37 °C for 20 min and terminated with 300 μl of methanol, and retinoids were extracted with 300 μl of hexane. The upper phase was removed and dried using a SpeedVac. The residue was dissolved in 200 μl of hexane, and 100 μl of this solution was analyzed by HPLC as described above.

Isomerase assays were performed as previously described (41, 42) with a few modifications. Reactions were carried out in 10 mM Tris/HCl buffer, pH 7.5, 1% bovine serum albumin, containing 1 mM ATP and 6 μM apo-cellular retinaldehyde-binding protein. Inhibition by test compounds was assessed by preincubating UV-treated RPE microsomes for 5 min at 37 °C with test compound delivered in 1 μl of DMF before the addition of apo-cellular retinaldehyde-binding protein and all-*trans*-retinol (10 μM). The same volume of DMF was added to control reactions. Experiments were performed three times in duplicates. For isomerization reaction assays in cell culture, NIH3T3 cells expressing LRAT and RPE65 were cultured in 6-well culture plates at a density of 1×10^6 cells/well for 20 h before each experiment. GM was removed, and 2 ml of fresh GM containing 10 μM all-*trans*-retinol and 3 μM test compound were added. Cells and medium were collected after 16 h of incubation. Samples were treated with 2 ml of methanol, homogenized, and saponified with 1 M KOH at 37 °C for 2 h prior to extraction with hexane. The resulting hexane phase was collected, dried using a SpeedVac, and redissolved in 250 μl of hexane, and retinoid composition was determined by normal phase HPLC as described above.

Inhibitor Administration and Extraction/Analysis of Retinoids from Mouse Eyes—Typically, all compounds tested in mice were delivered in 50 μl of tissue culture grade dimethylsulfoxide by intraperitoneal injection. Procedures related to the analysis of dissected mouse eyes, derivatization of retinals with hydroxylamine, and separation of retinoids have been described (14). Typically, two mice were used per assay, and assays were repeated three times.

Expression and Purification of Human RPE65—Full-length human RPE65 containing a C-terminal 1D4 tag was cloned into the pFastBac HT A plasmid, and the resulting construct was used to produce baculovirus according to the manufacturer's instructions (Invitrogen Bac-to-Bac handbook). For protein expression, 50 ml of high titer P3 baculovirus was added to 600 ml of cultured Sf9 cells at a density of 2×10^6 cells/ml, and the cells were shaken at 27 °C. After 36–48 h, cells were harvested by centrifugation and resuspended in 10 ml of PBS, pH 7.4, containing one dissolved tablet of EDTA-free complete protease inhibitors (Roche Applied Science). Cell suspensions were flash-frozen in liquid nitrogen and stored at −80 °C. Suspensions were thawed with 40 ml of 20 mM bis-tris-propane, pH 7.0, containing 150 mM NaCl, 10 mM 2-mercaptoethanol, 5% glycerol, 2 mM CHAPS, and one dissolved tablet of EDTA-free protease inhibitors (Roche Applied Science). Cells were disrupted by Dounce homogenization, and lysates were centrifuged at 145,000 × *g* for 30 min. The supernatant was collected, diluted 2-fold with lysis buffer, and loaded onto a 3-ml Talon resin (Clontech) column equilibrated with lysis buffer. The column was washed with 30 column volumes of 20 mM BTP, pH 7.0, 500 mM NaCl, 10 mM 2-mercaptoethanol, 5% glycerol, 2 mM CHAPS, and 5 mM imidazole. Protein was eluted with a

buffer consisting of 20 mM BTP, pH 7.0, 150 mM NaCl, 10 mM 2-mercaptoethanol, 5% glycerol, 2 mM CHAPS, and 150 mM imidazole, pH 7.0. Protein-containing fractions were pooled, TEV protease (43) was added at a concentration of 3% (w/w) (based on protein concentration), and mixtures were incubated at 4 °C for ~14 h to remove the N-terminal His_6 tag, and protein was purified further on a Superdex 200 gel filtration column. Fractions containing RPE65 were identified by immunoblotting. RPE65 preparations were >99% pure after gel filtration chromatography based on Coomassie- and silver-stained SDS-PAGE.

Tissue Extraction of Ret-NH_2 and N-Retinylamides—Mouse liver (1 g) was homogenized in 10 ml of 50 mM Tris/HCl buffer, pH 9.0, and 10 ml of methanol. The retinoids were extracted with 20 ml of hexane. The organic phase containing retinoids was collected, dried down in a SpeedVac, and resuspended in 0.5 ml of 20% ethyl acetate/hexane containing 0.5% ammonia in methanol. *N*-Retinylamides were separated on a normal phase HPLC column (Agilent-Si; 5 μm, 4.5 × 250 mm) by a solution of 20% ethyl acetate in hexane at a flow rate of 2 ml/min, whereas Ret-NH_2 was eluted with 100% ethyl acetate in the presence of 0.5% ammonia in methanol at a flow rate of 2.5 ml/min.

Mouse A2E Analysis—Two whole mouse eyes were homogenized and extracted twice in 1.0 ml of CH_3CN with a glass-glass homogenizer and dried using a SpeedVac. The residue was redissolved in 120 μl of 80% CH_3CN in H_2O with 0.1% trifluoroacetic acid, and 100 μl was analyzed by reverse phase HPLC with a C18 column (4.6 × 250 mm, 5 μm, Phenomenex, Torrance, CA) developed with a linear gradient of CH_3CN (0–100%) in H_2O with the addition of 0.1% trifluoroacetic acid at a 1.5 ml/min flow rate. Quantification of A2E and iso-A2E was performed by comparison with known concentrations of pure synthetic A2E and iso-A2E (44).

Expression and Purification of Human Serum RBP—Human RBP cDNA cloned into a pET3a expression vector was a gift from Dr. J. W. Kelly (Scripps Research Institute, La Jolla, CA). RBP expression in *Escherichia coli* was done as previously described (45). Briefly, RBP was expressed in BL-21 DE3 cells according to a standard protocol. Bacterial cells were harvested and lysed by osmotic shock. Insoluble material was pelleted, washed three times with 20 mM Tris/HCl buffer, pH 8.0, and solubilized in 7 M guanidine hydrochloride and 10 mM dithiothreitol. Buffer (25 mM Tris/HCl, pH 8.8) was added to dilute the guanidine hydrochloride concentration to 5.0 M. After overnight incubation, insoluble material was removed by ultracentrifugation (120,000 × *g*, 1 h, 4 °C), and the collected supernatant was used for the RBP refolding procedure. RBP was refolded by the dropwise addition of solubilized material to a mixture containing 25 mM Tris/HCl, pH 8.8, 0.3 mM cystine, 3.0 mM cysteine, 1 mM EDTA, and 1 mM all-*trans*-retinol delivered in ethanol at 4 °C. The reaction was carried out for 5 h at 4 °C with vigorous mixing. The precipitate was removed by ultracentrifugation (120,000 × *g*, 1 h at 4 °C), and the solution was dialyzed against 10 mM Tris/HCl buffer, pH 8.0, at 4 °C overnight, filtered, and loaded on a DE53 cellulose chromatography column. Refolded holo-RBP was eluted by a linear gradient of NaCl (0–300 mM) in 10 mM Tris/HCl buffer, pH 8.0. Collected fractions were examined by SDS-PAGE and UV-visible spectroscopy. Fractions containing RBP with an absorbance ratio at 280 nm/330 nm of 0.9 or higher were pooled, concentrated, and stored at −80 °C until further use.

Loading of Apo-RBP with Ret-NH_2—Apo-RBP was prepared by extracting all-*trans*-retinol into diethyl ether as described by Cogan *et al.* (46). The efficiency of all-*trans*-retinol extraction was monitored by recording the absorption spectra of the aqueous phase. For rebinding of Ret-NH_2 to RBP, a solution of apo-RBP (2 mg/ml) in 20 mM Tris/HCl, pH 8.0, was incubated for 2 h at 4 °C with 1 mM of Ret-NH_2 delivered in ethanol in the presence of 10% glycerol. The sample was diluted with 20 mM Tris/HCl buffer, pH 8.0, centrifuged and purified on a uno-Q ion exchange column. The presence of Ret-NH_2 bound to RBP was confirmed by measuring its absorbance spectrum after fast protein liquid chromatography purification.

Fluorescence Binding Assays—A spectrofluorometric technique was used to study the binding of Ret-NH_2 to RBP and RPE65. All measurements were performed on a PerkinElmer Life Sciences LS55 model fluorometer (Waltham, MA). Binding of Ret-NH_2 was evaluated by monitoring the quenching of protein fluorescence at increasing concentrations of ligand. With the excitation wavelength set at 285 nm, emission spectra were recorded from 300 to 520 nm with bandwidths for excitation and emission fixed at 10 nm. Titrations were carried out at 20 °C in 20 mM Tris/HCl buffer, pH 7.6, containing 50 mM NaCl and 5% glycerol (v/v). Ret-NH_2 was delivered in DMF so that the final volume of DMF did not exceed 0.5% of the sample's total volume. All binding data were corrected for background and self-absorption of excitation and emission light. Using Prism 3.02 (GraphPad Software, Inc., San Diego, CA), we calculated apparent K_d values by nonlinear regression for a single binding site with the equation $Y = B_{max} \times X/(K_d + X)$, where B_{max} is the maximal binding, and K_d is the concentration of ligand required to reach half-maximal binding.

Retinoid Uptake Assays—Twenty hours prior to an experiment, NIH3T3 cells expressing LRAT or LRAT and STRA6 were cultured in 6-well culture plates at a density of 1×10^6 cells/well. Cells were washed with 137 mM NaCl, 67 mM potassium phosphate, 2.7 mM KCl, pH 7.4, and serum-free medium containing either RBP-Ret-NH_2 or free Ret-NH_2 dissolved in DMF was added. After a 16-h incubation at 37 °C, cells were washed twice with 137 mM NaCl, 67 mM potassium phosphate, 2.7 mM KCl, pH 7.4, harvested, and extracted with 1 volume of methanol followed by 2 volumes of hexane. The entire hexane phase was collected, dried down in a SpeedVac, and redissolved in 250 μl of hexane. Retinoids were analyzed by normal phase HPLC on a Hewlett Packard 1100 series HPLC system. *N*-Retinylamides were separated on an Agilent-Si column (4.6 × 250 mm, 5 μm) equilibrated with 20% ethyl acetate in hexane and eluted with the same solution at a flow rate of 2 ml/min (29, 30).

Electroretinograms (ERGs)—ERG recordings were done as previously described (47, 48).

RESULTS

A Protonatable Amino Group Is Required for High Potency Visual Cycle Inhibition—To evaluate the effects of different classes of inhibitors on 11-*cis*-retinol production in RPE micro-

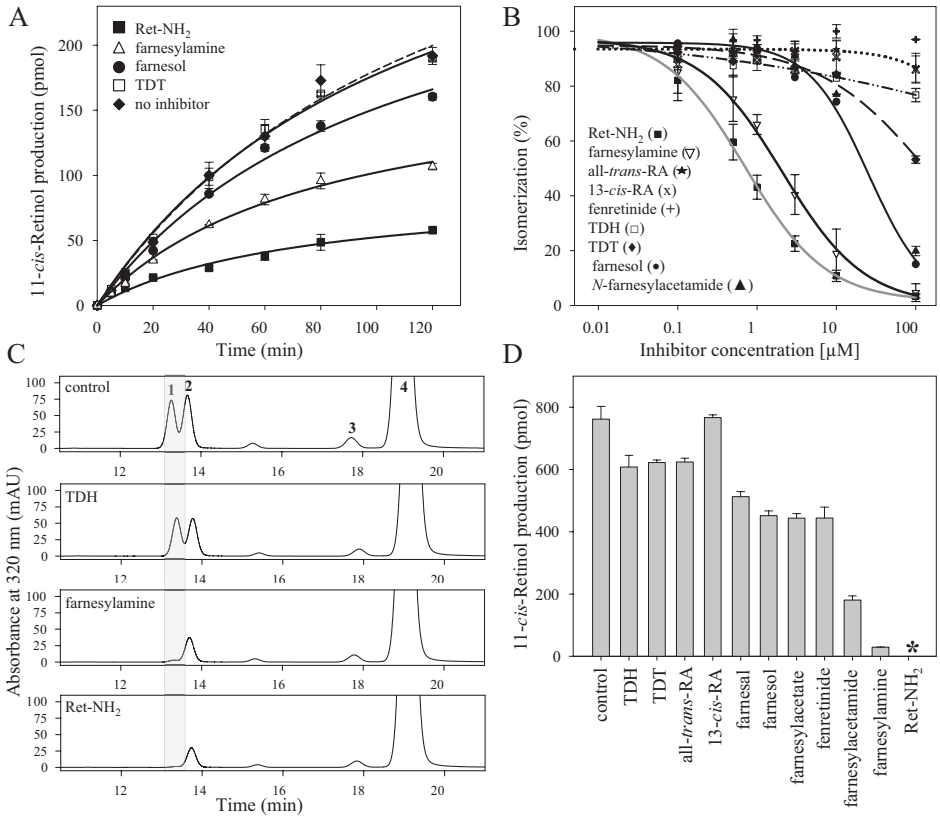

FIGURE 2. **Inhibition of 11-*cis*-retinol production by visual cycle inhibitors.** RPE microsomes were preincubated for 5 min with each compound tested at a concentration of 3 μM prior to initiation of the isomerization reaction through the addition of 10 μM all-*trans*-retinol and 6 μM apo-cellular retinaldehyde-binding protein. *A*, the progress of the isomerization reaction measured as an increase of 11-*cis*-retinol concentration with time. *B*, dose-dependent effects of inhibitors on 11-*cis*-retinol production by RPE microsomes. Assays were performed at 30 °C for 1 h. *C*, HPLC chromatograms indicating a robust isomerization reaction in NIH3T3 cells expressing RPE65 and LRAT. Cells were incubated with 10 μM all-*trans*-retinol in growth medium for 16 h prior to organic extraction. Supplementation of the growth medium with 3 μM Ret-NH_2 or farnesylamine resulted in nearly complete inhibition of 11-*cis*-retinol production. Peaks were identified based on elution time and absorbance spectra that were identical with synthetic standards (*1*, 11-*cis*-retinol; *2*, 13-*cis*-retinol; *3*, 9-*cis*-retinol; *4*, all-*trans*-retinol). *D* shows amounts of 11-*cis*-retinol found in samples treated with 3 μM concentrations of the test compounds (*, below detection levels). mAU, milliabsorbance units.

somes, we performed *in vitro* isomerization activity assays in the presence of 3 μM Ret-NH_2, farnesylamine, or TDT (Fig. 2*A*). The isomerization reaction, monitored by an increase of 11-*cis*-retinol concentration with time, was significantly slowed when Ret-NH_2 or farnesylamine was added, whereas TDT had no measurable inhibition. Farnesol used to control nonspecific effects of the isoprenoid moiety on the isomerization reaction, showed only mild inhibition, as expected. To characterize the inhibitory properties of these and other compounds further, we performed a series of experiments with increasing concentrations (range 0–100 μM) of test inhibitors (Fig. 2*B*). Ret-NH_2 again was the most potent inhibitor with an IC_{50} = 650 nM, a value in good agreement with previously published results (29). Farnesylamine exhibited lower inhibitory activity in the isomerization reaction, with an IC_{50} = 1,200 nM. Fenretinide, TDH, TDT, 13-*cis*-RA, and all-*trans*-RA had much weaker inhibitory effects.

The above findings were verified by cell culture experiments. NIH3T3 cells stably expressing LRAT and RPE65 were treated with 10 μM all-*trans*-retinol in addition to 3 μM of each putative inhibitor for 16 h prior to cell homogenization, saponification, and retinoid extraction. HPLC analysis revealed robust production of 11-*cis*-retinoids in nontreated cells, whereas the addition of either Ret-NH_2 or farnesylamine dramatically reduced isomerase activity (Fig. 2, *C* and *D*). RA isomers as well as TDH and TDT had no significant effect on this activity, although fenretinide exhibited partial inhibition similar to that of farnesol. Thus, the above results correlate well with our *in vitro* data. The only exception was *N*-farnesylacetamide that showed much higher inhibitory potency in the tissue culture experiments (Fig. 2*D*). This difference might be explained by hydrolysis of *N*-farnesylacetamide to farnesylamine occurring during the cellular incubation. A similar effect was reported for *N*-retinylamides in previous studies (30). Together, these observations demonstrate that a protonatable amino group is a prerequisite for the efficacy of retinoid isomerase inhibitors (29). This idea is also consistent with the proposed molecular mechanism for the isomerization reaction (reviewed in Ref. 49).

Ret-NH_2 Blocks the Enzymatic Activity of RPE65—Identification of RPE65 as a retinoid isomerase in bovine RPE (5–7) in addition to Ret-NH_2 as an efficient isomerase inhibitor in NIH3T3 cells robustly expressing LRAT and RPE65 suggests a direct interaction of the positively charged Ret-NH_2 with RPE65. Because a previously published observation failed to reveal a specific effect of Ret-NH_2 on RPE65 activity in RPE microsomes solubilized in potentially destabilizing detergent (29), we avoided the use of detergents in the present experiments. Instead, RPE65 was expressed in Sf9 cells and purified to homogeneity, and putative binding of Ret-NH_2 was tested by fluorescence methodology. As shown in Fig. 3*A*, incubation of Ret-NH_2 with RPE65 led to an exponential decay in protein fluorescence. This decay displayed a saturable binding isotherm (Fig. 3*B*), providing an average binding K_d of 80 nM. This result identifies RPE65 as a primary target for amine-based inhibitors of retinoid isomerization, a finding consistent with available information about the ocular effects of these compounds. Although Ret-NH_2 can be metabolized by LRAT to form *N*-retinylamides (30), all-*trans*-retinol remains a preferred substrate for this enzyme, and consequently we observed no influence of Ret-NH_2 on retinyl ester formation, either *in vitro* or *in vivo* (29, 30). Importantly, neither Ret-NH_2 nor farnesylamine interfered with RDH activities (data not shown), as was reported for 13-*cis*-RA (50). Thus, RPE65 appears to be the

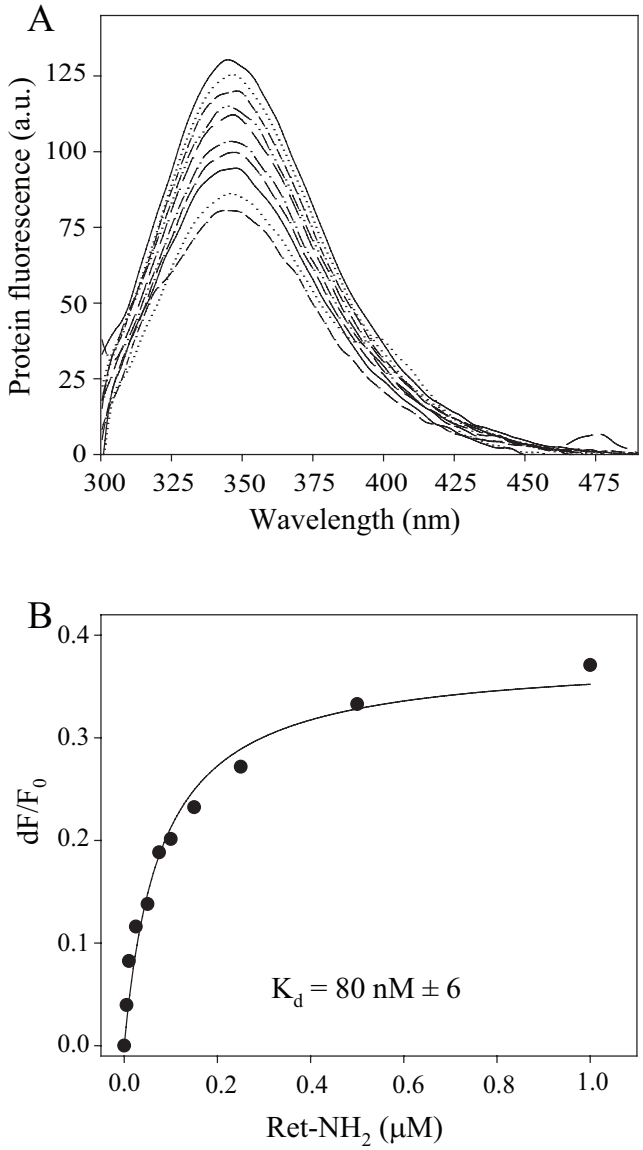

FIGURE 3. **Binding of Ret-NH_2 to RPE65 determined by quenching of protein fluorescence.** Purified RPE65 was diluted in 20 mM Tris/HCl buffer, pH 7.6, containing 50 mM NaCl and 5% glycerol (v/v) to a final concentration of 0.05 μM. Increasing quantities of Ret-NH_2 were added in 1-μl aliquots of DMF to 2 ml of total sample. After each addition, the titrated solution was mixed and incubated for 1 min prior to excitation at 285 nm and recording of emission spectra. *A*, fluorescence spectra of RPE65 recorded upon the addition of increasing concentrations of Ret-NH_2 (0–1 μM). *B*, changes in maximum emission in response to increasing Ret-NH_2 concentrations were monitored at 345 nm; corrected for background, dilution, and inner filter effect; and used to estimate the apparent K_d values shown. *a.u.*, arbitrary units; *F*, protein fluorescence.

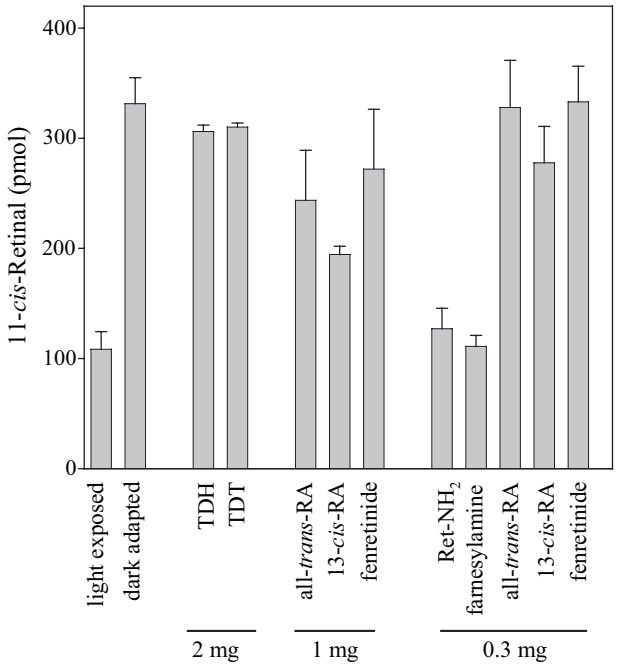

FIGURE 4. **Comparison of 11-*cis*-retinal regeneration in mice treated with selected visual chromophore inhibitors.** Dark-adapted mice were given the shown dose of inhibitor by intraperitoneal injection 4 h before they received a bleach for 20 min at 150 candela m^{-2} in a Ganzfeld chamber. Regeneration of 11-*cis*-retinal continued for 4 h in the dark, after which ocular retinoids were extracted and separated by normal phase HPLC as described under "Materials and Methods."

primary target for Ret-NH_2 action that disrupts the visual cycle in the RPE.

Comparison of the Effects of Ret-NH_2, Farnesylamine, and Other Inhibitors on the Retinoid Cycle in Vivo—Some of the tested compounds might possibly have mechanisms of action other than direct modulation of RPE65 activity. Therefore, we further evaluated the inhibitory doses and potency of these compounds in mice. Animals were treated with one of three doses of an inhibitor by intraperitoneal injection. Then they were exposed to intense light and subsequently were dark-adapted, and the retinoid composition of the eyes was analyzed 4 h later. As expected, effects of the visual cycle inhibitors varied markedly (Fig. 4). TDH and TDT had the least effect on visual chromophore regeneration, although they were given at the highest dose (2 mg/animal). 13-*cis*-RA, all-*trans*-RA, and fenretinide suppressed visual cycle intermediate regeneration by 30–50% under our experimental conditions. But both Ret-NH_2 and farnesylamine produced the greatest inhibition, implying that these compounds achieve therapeutic efficacy at the lowest doses *in vivo* (Fig. 4). Because the rate of absorption and delivery to the eyes may differ among tested compounds, we examined the effects of each inhibitor (1 mg) on 11-*cis*-retinal production over a wide (48 h) time frame (Fig. 5, *A* and *B*). With all-*trans*-RA, 13-*cis*-RA, and fenretinide, inhibition was detectable 2 h after compound administration and lasted up to 7 h postinjection. In contrast, Ret-NH_2 completely blocked the visual cycle for more than 18 h. Data obtained from HPLC analyses were consistent with electrophysiological measurements shown in Fig. 5, *C* and *D*. Single flash ERG a-wave and b-wave responses plotted as a function of varying light intensities were recorded for control and treated animals 5 and 16 h after bleach, respectively. Significant attenuation of these responses in Ret-NH_2-treated mice was sustained 16 h after bleach. 13-*cis*-RA-treated mice showed a mild but significant reduction of ERG responses at 5 h but no significant difference from controls at 16 h after bleach (***, $p < 0.0001$, one-way analysis of variance). No significant changes in ERG responses were seen in TDH-treated mice under these experimental conditions.

Direct comparison of Ret-NH_2 and farnesylamine indicates that these compounds have similar inhibitory potency occurring at the relatively low dose of 0.1 mg/animal. However,

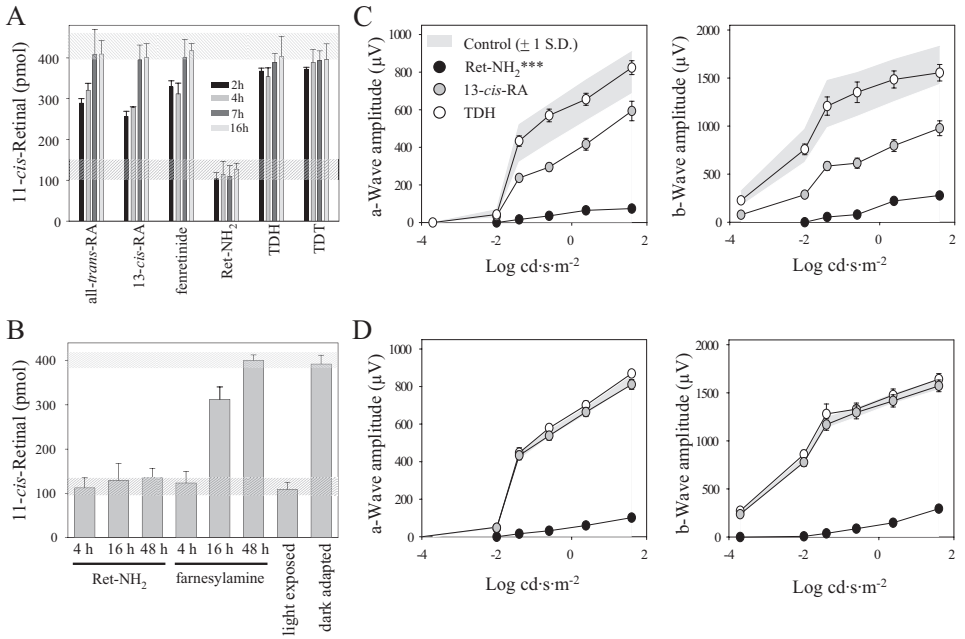

FIGURE 5. **Time course of 11-*cis*-retinal regeneration in mice given visual cycle inhibitors.** *A*, 1 mg of each tested compound was given to mice by intraperitoneal injection as described under "Materials and Methods." After exposure to light sufficient to bleach 80% of rhodopsin, animals were left in the dark for 4–16 h. Amounts of 11-*cis*-retinal within the dark-adapted eyes were determined by HPLC. Levels of visual chromophore in dark-adapted (*top*) and bleached (*bottom*) animals are shown by *dashed bars*. *B*, differences in duration of the inhibitory effects between Ret-NH_2 and farnesylamine at a dose of 0.1 mg/mouse. *C* and *D* represent single-flash ERG responses of increasing intensity by untreated control mice and mice treated with either Ret-NH_2, 13-*cis*-retinoid, or TDH. Mice were dark-adapted for 5 h (*C*) and 16 h (*D*) after bleaching. Serial responses to increasing flash stimuli ware plotted as a function of a- and b-wave responses *versus* varying light intensities under dark-adapted conditions. Attenuation of ERG responses was retained by Ret-NH_2-treated mice 16 h after bleach. *cd*, candela.

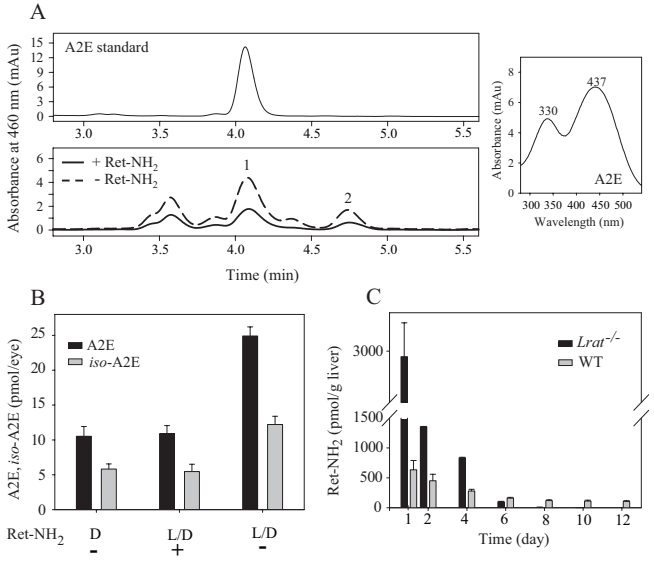

FIGURE 6. **Effect of Ret-NH_2 on A2E accumulation in *Abca4*$^{-/-}$ mice and comparison of the inhibitor clearance in WT and LRAT-deficient mice.** *A*, representative HPLC chromatogram of A2E detected in a Ret-NH_2-treated mouse, compared with a control mouse treated with vehicle only. One-month-old *Abca4*$^{-/-}$ mice were gavaged with Ret-NH_2 (1 mg) in 150 μl of vegetable oil every 2 weeks for 2 months and were analyzed 1 week after the last gavage at 3 months of age. Mice were maintained in the complete darkness (*D*) or in a 12 h/12 h dark/light (*L/D*) cycle (~10 lux). A2E and iso-A2E levels were examined by reverse phase HPLC as described under "Materials and Methods." Peaks were identified based on elution time and UV-visible spectra (*right*). *Peak 1*, A2E; *peak 2*, iso-A2E. *B*, quantification of A2E and iso-A2E found in the eyes. The *error bars* indicate the S.E. ($n = 3$; *, $p < 0.0001$; Ret-NH_2-treated *versus* Ret-NH_2-untreated). *C*, comparison of Ret-NH_2 levels over time in livers of WT and *Lrat*$^{-/-}$ mice gavaged with a single dose (1 mg) of Ret-NH_2. *mAU*, milliabsorbance units.

Ret-NH_2 inhibition continued over several days (47), whereas farnesylamine reduced 11-*cis*-retinal production for less than 20 h (Fig. 5*B*). This result could be explained by efficient amidation of Ret-NH_2 catalyzed by LRAT. *N*-Retinylamides are storage forms of Ret-NH_2 that accumulate within the RPE (30), where they are protected from being rapidly metabolized. Evidence supporting this idea comes from comparing Ret-NH_2 metabolism between WT and *Lrat*$^{-/-}$ mice. The amount of Ret-NH_2 measured in the liver of LRAT-deficient mice declined rapidly to an undetectable level within 6 days after gavage with 1 mg of the inhibitor. In contrast and despite formation of *N*-retinylamides in WT mice, Ret-NH_2 persisted at a constant level in these animals for up to 2 weeks (Fig. 6*C*). Thus, slow hydrolysis of amides back to the amine form appears to provide a constant supply of inhibitor that accounts for its prolonged therapeutic effect.

Interestingly, administration of effective doses of Ret-NH_2 did not produce toxic effects in mice (47). In contrast, doses of farnesylamine over 0.5 mg/animal produced significant toxicity manifested by vellicated coats, dyspnea, and poor mobility. These toxic effects may relate to the reported inhibition of farnesyl/protein transferases that modulate cellular activities controlled by a variety of signaling proteins, including small G-proteins (51, 52). Farnesylamine also is a competitive inhibitor of the mitochondrial outer membrane enzyme, monoamine oxidase B, that is involved in controlling levels of neurotransmitter amines (53, 54).

Effect of Ret-NH_2 on A2E Accumulation in Abca4$^{-/-}$ *Mice*—Inhibition of the visual cycle by Ret-NH_2 is accompanied by reduced lipofuscin fluorophore accumulation. Administration of the inhibitor at 1 mg/animal every 2 weeks for 2 months reduced production of A2E and iso-A2E in *Abca4*$^{-/-}$ mice to levels found in animals kept in darkness (Fig. 6, *A* and *B*). This result demonstrates that blocking RPE65 activity is an effective way to attenuate the rate of A2E accumulation *in vivo*. Moreover, the dose of Ret-NH_2 required to evoke therapeutic effects in mice is much lower compared with 13-*cis*-RA or fenretinide (17, 18).

Delivery of Ret-NH_2 and Fenretinide to the Eye Is Not RBP- or STRA6-dependent—Recent identification of the multitransmembrane protein, STRA6, as a RBP receptor within RPE cells (55) has important implications for understanding how RBP-bound retinoid compounds are delivered to the eye. To elucidate the roles of RBP and STRA6 in Ret-NH_2 transport, we examined Ret-NH_2 binding to RBP and its uptake by cells

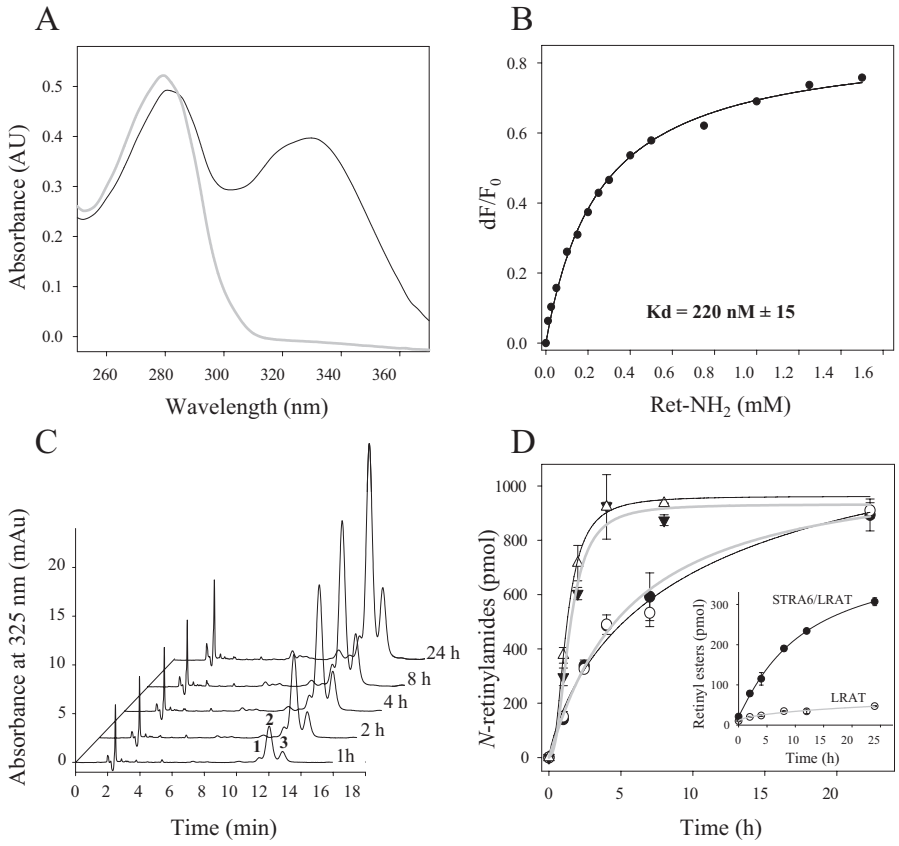

FIGURE 7. **Interaction of Ret-NH_2 with RBP and its uptake by cells expressing LRAT and STRA6.** *A*, apo-RBP was prepared by extraction of holo-RBP with diethyl ether. Completeness of ligand absence was monitored by UV-visible spectroscopy (*gray line*). Incubation of apo-RBP with Ret-NH_2 and repurification on a fast protein liquid chromatography ion exchange column produced Ret-NH_2-RBP with a UV-visible spectrum characterized by two maxima, one at 280 and the other at 330 nm (*black line*), corresponding to protein and retinoid absorbance, respectively. Absorption at 330 nm was taken to indicate binding of Ret-NH_2 to RBP. The apparent K_d value was established by fluorescence titration of apo-RBP (0.2 μM) with increasing concentrations of Ret-NH_2 in 20 mM Tris/HCl buffer, pH 7.6, and 50 mM NaCl, as shown in *B*. *C*, uptake of Ret-NH_2 bound to RBP by NIH3T3 overexpressing LRAT and STRA6. Efficiency of uptake was taken as the amount of all-*trans*-*N*-retinylamides extracted from the cells. Chromatograms represent normal phase HPLC separation of *N*-retinylamides extracted from cells collected at different time points after incubation with RBP-Ret-NH_2. *Peaks 1*, *2*, and *3* correspond to all-*trans*-*N*-retinylamides containing of C18, C16, and C14 acyl groups, respectively. *D*, Ret-NH_2 uptake by NIH3T3 cells expressing STRA6 and LRAT (*filled shapes*) or LRAT alone (*open shapes*). Incubation of cells with Ret-NH_2 bound to RBP (*circles*) at a concentration of 8 μM in serum-free Dulbecco's modified Eagle's medium revealed no difference in uptake efficiency between the two cell lines. A higher rate of retinoid accumulation was observed when both cells lines were incubated with "free" Ret-NH_2 at the same concentration (*triangles*). A control experiment (*inset*) shows robust retinol uptake (assayed as retinyl esters) by STRA6/LRAT cells incubated with holo-RBP as compared with cells expressing LRAT alone. *AU*, absorbance units.

expressing STRA6. As shown by UV-visible spectroscopy and fluorescence measurements, Ret-NH_2 bound to apo-RPB with high affinity (K_d = 220 nM) at physiological pH (Fig. 7, *A* and *B*). This value is comparable with the previously reported affinity of human all-*trans*-retinol for apo-RBP (K_d = 150 nM) (46). Therefore, RBP loaded with Ret-NH_2 and repurified on an ion exchange column was used for our uptake assays. Because LRAT activity is required for efficient retinoid storage within cells (32, 56), NIH3T3 cells overexpressing LRAT and STRA6 were incubated with RBP-Ret-NH_2 added to the medium. The cells were washed, harvested, and extracted, and their retinoid content was examined by normal phase HPLC. Uptake efficiency was assessed as the amount of *N*-retinylamides found in these cells over time (Fig. 7*C*). In contrast to control experiments wherein uptake of all-*trans*-retinol from holo-RBP was 10-fold higher in cells expressing STRA6/LRAT compared with cells expressing only LRAT (Fig. 7*D*, *inset*), the rate of Ret-NH_2 uptake from Ret-NH_2-loaded RBP was indistinguishable between these two cell lines (Fig. 7*D*). Interestingly, the rate of *N*-retinylamide accumulation by cells overexpressing LRAT alone was comparable with the rate of all-*trans*-retinol uptake by cells overexpressing STRA6/LRAT. Moreover, Ret-NH_2 prebound to RBP was taken up much more slowly by these cell types than free Ret-NH_2 when identical concentrations were added to the medium. These observations indicate that the RBP/STRA6-dependent mechanism does not enhance Ret-NH_2 transport across cell membranes as it does for retinol bound to RBP. The relatively high rate of *N*-retinylamide accumulation upon incubation of cells with RBP-Ret-NH_2 suggests that charged Ret-NH_2 might partition between the binding protein and cell membranes.

The role of RBP in ocular delivery of retinoids was investigated further with *Rbp* knock-out mice. Both Ret-NH_2 and fenretinide have been shown to bind to RBP. Moreover, fenretinide reduces RBP-transthyretin complex formation, resulting in increased renal filtration of free RBP and decreased levels of serum RBP that in turn reduce the flux of retinol to the eye. This mechanism is considered to account for the reduced retinoid cycling rate observed in fenretinide-treated patients (18). To test this hypothesis, dark adapted RBP-deficient mice were gavaged 4 h prior to light exposure with either 1 mg of fenretinide or 1 mg of Ret-NH_2. After 4 h of dark adaptation, the animals were sacrificed, and levels of 11-*cis*-retinal and other visual retinoids were quantified in the eye by HPLC. $Rbp^{-/-}$ mice had slightly higher levels of regenerated visual chromophore (20% of the control level) than WT mice (10%) (Fig. 8, *A* and *B*). Concomitantly, the uptake of Ret-NH_2, determined by the amount of *N*-retinylamides found in the eyes, was 25% higher in WT *versus* knock-out mice (Fig. 7*C*). Although these differences were statistically significant, they suggest a relatively minor role for RBP in Ret-NH_2 transport into the eye *in vivo*. The same seems to be true for fenretinide. Administration of the latter compound lowered 11-*cis*-retinal production by 20% in both $Rbp^{-/-}$ and WT mice (Fig. 8, *A* and *B*). Moreover, no differences in fenretinide levels in the eyes of treated animals were found (Fig. 8*C*).

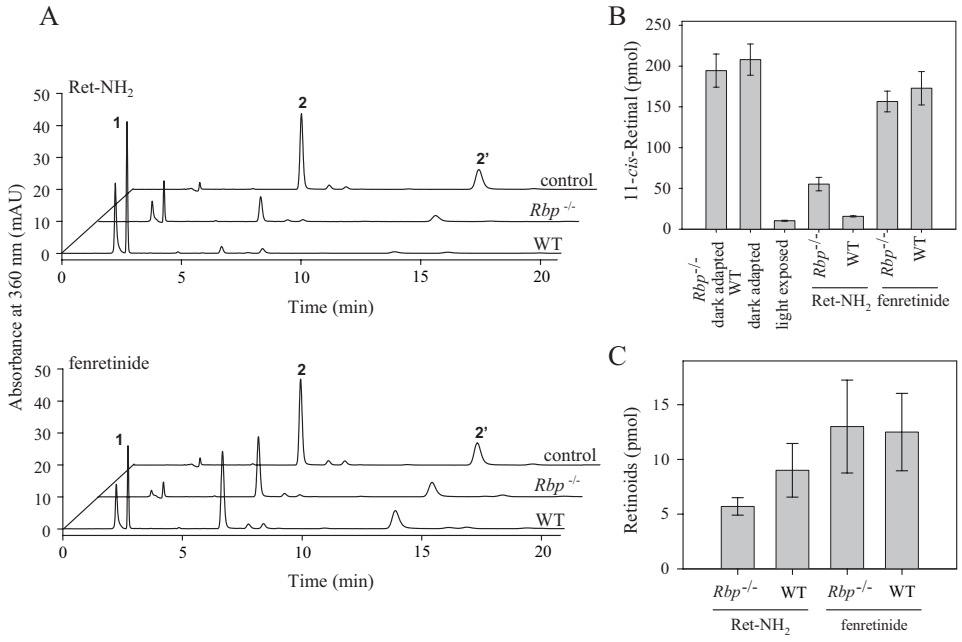

FIGURE 8. **Role of RBP in Ret-NH$_2$ delivery to the eye.** *Rbp*$^{-/-}$ and WT mice received a gavage dose of 1 mg of Ret-NH$_2$ or fenretinide in oil by gastric gavage. Four hours later, mice were exposed to strong light calculated to bleach 90% of rhodopsin and then were left in the dark to allow visual chromophore regeneration. *A*, chromatograms of retinoids from mouse eyes. *Peak 1*, all-*trans*-retinyl esters; *peak 2*, 2′-11-*cis*-retinal oximes (*syn*, *anti*). *B*, quantification of 11-*cis*-retinal oximes detected in ocular samples from *A*. *C*, concentrations of *N*-retinylamides and fenretinide found in the eyes of RBP-deficient and WT mice. Compounds were detected in hexane extracts prepared from dissected eyes by normal phase HPLC with 30% ethyl acetate/hexane used as the solvent at a flow rate of 1.4 ml/min.

DISCUSSION

Overproduction of fluorescent lipofuscin pigment (*i.e.* dihydro-*N*-retinylidene-*N*-retinylphosphatidylethanolamine) in photoreceptor cells and its subsequent conversion and accumulation in the form of A2E in RPE, as indicated by fundus autofluorescence, precedes macular degeneration and visual loss in age-related macular degeneration and Stargardt disease (57). Strong autofluorescence within the retina also is observed in patients with Best vitelliform macular dystrophy and a subset of patients diagnosed with cone-rod dystrophy (58). The well studied cytotoxic effects of A2E are manifested by induced release of proapoptotic proteins from the mitochondria (59), impaired degradation of phospholipids from phagocytosed outer segments (21), a detergent-like destabilization of cellular membranes (60), and sensitization of RPE cells to light damage (61, 62). As a result of these changes, RPE cells begin to function abnormally and lose their ability to support photoreceptor activity, a scenario that eventually leads to photoreceptor degeneration (63). Because A2E accumulation causes retinal and macular degeneration, inhibition of lipofuscin pigment formation appears to be a rational therapeutic approach for slowing the progression of visual loss. The utility of this strategy is underscored by the observation that *Abca4*$^{-/-}$ mice (an animal model of human Stargardt disease) raised in total darkness have reduced levels of A2E compared with animals subjected to cyclic light exposure (18, 19, 64). The precursor of A2E, dihydro-*N*-retinylidene-*N*-retinylphosphatidylethanolamine, is a product of phosphatydyloethanolamine condensation with two molecules of all-*trans*-retinal that is located in the ROS (63). Thus, a decrease in all-*trans*-retinal production should slow the rate of A2E accumulation. The most effective way to influence light-dependent formation of all-*trans*-retinal is to modulate visual chromophore regeneration by pharmacological inhibition. To accomplish this, there is a need to identify, develop, and characterize effective, selective, and nontoxic inhibitors of visual chromophore regeneration that can be efficiently delivered to the eye. In this study, we evaluated the therapeutic efficacy and mode of action of several compounds claimed to be visual cycle inhibitors that might be useful for the treatment of degenerative retinal diseases.

Relationship between Mode of Action and Therapeutic Approaches—We investigated four chemical classes of visual cycle inhibitors to establish their inhibitory efficacy, potency, and specificity *in vitro* in cell culture and *in vivo* (Fig. 1). Among the compounds studied, Ret-NH$_2$ and farnesylamine were the most effective inhibitors of 11-*cis*-retinal production in each of these experimental systems (Figs. 2, 5, and 6). Similarities between the structures and inhibitory properties of these two compounds suggest the same mechanism of action. RPE65 is the likely target for Ret-NH$_2$ action, not only because Ret-NH$_2$ had high inhibitory potency toward this enzyme (Fig. 3) but also because it failed to inhibit either LRAT or rod and cone RDH activities. Together, these results indicate a highly specific and sensitive molecular mechanism through which Ret-NH$_2$ slows 11-*cis*-retinal formation by interfering with the essential actions of RPE65 in the visual cycle.

We found that 13-*cis*-RA had only a minor effect on retinoid isomerization *in vitro* and in cell culture assays. This contradicts previous reports proposing that 13-*cis*-RA inhibits visual chromophore regeneration by binding to RPE65 (28, 65). An alternative explanation is that 13-*cis*-RA inhibits 11-*cis*-RDH and all-*trans*-RDH in RPE and rod outer segments, respectively (27, 40). The greater than 10-fold lower K_i value reported for 13-*cis*-RA inhibition of 11-*cis*-RDH activity as compared with that of all-*trans*-RDH suggests that the latter RPE-localized protein may be the predominant target for 13-cis-RA. A relatively weak effect of 13-*cis*-RA on visual chromophore production was observed *in vivo* (Figs. 4 and 5), but this might be due to tight control of RA levels in cells by its rapid clearance through oxidation by CYP26 enzymes (66). 13-c*is*-RA also was shown to isomerize spontaneously to its all-*trans*-isomer *in vivo*; this would decrease its half-life and might limit its effects on the visual cycle *in vivo* (reviewed in Ref. 67). Although administration of 13-*cis*-RA to *Abca4*$^{-/-}$ mice prevents formation of A2E, high doses of this compound are needed to inhibit the visual

cycle. Moreover, the toxicity of 13-*cis*-RA renders it unsuitable for long term treatment of patients with retinal degenerative diseases (17, 20).

It is unclear by which mechanism fenretinide influences visual chromophore formation in the eye. It does not block 11-*cis*-retinol production by RPE microsomes or in cultured cells. Moreover, it fails to inhibit LRAT or RDH activity tested by *in vitro* assays (Fig. 2). The only measurable effect of this retinoid on 11-*cis*-retinal production was observed in mice (18) (Figs. 4 and 5). Based on clinical studies, one proposed action of fenretinide is to reduce circulating levels of retinol by competitive binding to RBP. This would lower the pool of retinol available to support vision, which in turn would decrease A2E formation (68). But in light of our finding that acute exposure to this retinoid produced modest inhibition of the retinoid cycle in WT and $Rbp^{-/-}$ mice, this mechanism cannot account for ocular effects observed after short term treatment *in vivo*. Only after chronic administration (several months) of fenretinide did patients show night blindness. These observations in humans suggest that fenretinide does not act directly to inhibit the visual cycle. Thus, the primary target of fenretinide action remains unclear. Uncharged compounds, such as TDH and TDT, containing unsaturated and uncharged long-chain esters lacked inhibitory efficacy in both our *in vivo* and *in vitro* assays.

Role of RBP in Visual Inhibitor Transport—The eye relies on RBP to ensure sufficient retinoid delivery from the circulation to sustain visual function. Mice with a knock-out mutation in the *Rbp* gene manifest visual impairment early in life (69). RBP is primarily synthesized in and secreted from the liver, by recruiting all-*trans*-retinol from the body's main retinoid storage organ (70). Retinol uptake by the RPE involves a multitransmembrane cell surface receptor for RBP, encoded by the *STRA6* gene (55). Retinoid requirements for tissues other than the eye can be fully satisfied by alternatives to RBP transport that involve chylomicrons or albumin-mediated delivery (35). Thus, a RPB/STRA6-dependent retinoid uptake pathway might constitute a highly specific way to target visual inhibitors to the eye. Here we tested uptake of two compounds that bind to RBP, Ret-NH_2 and fenretinide, by using a cell culture system and RBP-deficient mice. Because no difference in the rate of Ret-NH_2 uptake was observed in cells expressing STRA6/LRAT *versus* LRAT alone, RBP/STAR6-dependent transport of synthetic retinoids cannot be the major pathway of Ret-NH_2 delivery to the eye (Fig. 7). Accumulation of *N*-retinylamides by cells incubated with Ret-NH_2 prebound to RBP also was slower than accumulation by cells exposed to free Ret-NH_2 in the medium. Additionally, levels of 11-*cis*-retinal and amounts of Ret-NH_2 or fenretinide found in the eyes of $Rbp^{-/-}$ and WT mice treated with these compounds were comparable (Fig. 8).

Transport of synthetic retinoids depends on the hydrophobicity of these compounds. Because Ret-NH_2 and fenretinide are less hydrophobic than retinyl esters or retinol, the former compounds most likely are not incorporated into chylomicrons but rather are absorbed into the portal circulation and transported bound to albumin. Like RA and retinol, synthetic retinoids may dissociate from albumin and cross cell membranes by passive nonionic diffusion (71). For polar retinoids like Ret-NH_2, uptake also can be driven by differences in pH between blood (pH 7.4) and cytoplasm (pH ~ 7.0). The pK_a value for the amino group of Ret-NH_2 is about 7.0. Thus, protonation of Ret-NH_2 might selectively concentrate it inside a cell. Another way for ensuring efficient tissue recruitment of this compound is through esterification or amidation by LRAT. These processes would lead to active partitioning of Ret-NH_2 from the circulation into tissues and the establishment of a slowly metabolized storage pool of prodrug in the eye and liver (30).

Function of the Protonatable Amino Group in the Structure of Visual Cycle Inhibitors—The RPE65 crystal structure has not been determined to date, and the only information about the RPE65 isomerization reaction mechanism is derived from biochemical studies. A variety of published data suggest that this reaction involves a carbocation mechanism. Protonation of retinoid followed by an elimination reaction leads to delocalization of the positive charge throughout the conjugated double bonds, thereby lowering the energy requirement for the conformational change needed for 11-*cis*-retinoid formation (3, 72) (reviewed in Ref. 49). Ret-NH_3^+ might mimic the transition state proposed for this carbocation mechanism, and hence any modifications of the amino group would reduce the potency of this inhibitor. Conversely, the β-ionone ring is not crucial for the inhibitory properties of Ret-NH_2, because acyclic Ret-NH_2 derivatives also show inhibitory activity (29). This observation opens the possibility of designing nonretinoid hydrophobic primary amine inhibitors targeting RPE65. One such compound with high inhibitory potency is farnesylamine (Figs. 2, 5, and 6), but farnesylamine interferes with other enzymatic reactions utilizing carbocation mechanisms. This difficulty is well illustrated by the prenyltransferases that include three classes of enzymes: isoprenyl pyrophosphate synthases, protein prenyltransferases, and terpenoid cyclases (73, 74) (reviewed in Ref. 75). The prenyltransferases are widely distributed in nature and support a variety of important biological functions related to cell growth and survival, motility, cytoskeletal regulation, intracellular transport, secretion, and cell signaling (76, 77). Inhibition by farnesylamine of both RPE65 and protein prenyltransferases is another argument for a carbocation mechanism for retinoid isomerization. However, the similarity of transition states with those of vital endogenous compounds creates a redundancy in the mechanism of action of farnesylamine that leads to its undesirable side effects and high toxicity.

Role of Amide Formation in Lowering Amine Toxicity—The function of LRAT is to allow tissues to accumulate and store retinol (32, 56). Formation of retinyl esters also reduces the pool of retinol that can be oxidized, thereby preventing overproduction of RAs (78). The role of LRAT in detoxifying retinoids with an alcohol or amino functional group can be used to therapeutic advantage. Conversion of Ret-NH_2 into *N*-retinylamides protects the relatively reactive amino group and reduces the polarity of this compound, allowing its storage in lipid droplets within the eye, liver, and possibly in other tissues. Thus, this amidation acts as a protective mechanism against potential toxicity and also contributes to the prolonged therapeutic effect of Ret-NH_2 compared with the other visual cycle inhibitors we studied (Fig. 6*C*). Unfortunately, LRAT is highly specific for retinoid derivatives, so its benefits are limited to these compounds (79). Hydrophobic alcohols like geraniol and tetradeca-

nol are poor LRAT substrates, and nonretinoid amines like farnesylamine are even worse than their alcohol analogs. The selectivity of LRAT for retinoids is clearly evident from comparing the inhibitory properties of Ret-NH_2 and farnesylamine. Although both compounds exhibit similar inhibitory potency *in vitro* and in cell culture studies, farnesylamine is far more toxic and remains biologically active for a significantly shorter period *in vivo* than Ret-NH_2.

In summary, our findings demonstrate that Ret-NH_2 is the most potent and specific visual cycle inhibitor among the studied compounds. Ret-NH_2 enters the eye through an RBP- and STRA6-independent mechanism but requires LRAT activity in the ocular tissue for its prolonged therapeutic effect. A drug like Ret-NH_2, with a well defined highly specific molecular target and a low effective dose, is less likely to cause toxicity because of nonspecific interactions. Ret-NH_2 is the first visual cycle inhibitor that, based on the proposed mechanism of retinoid isomerization, was designed specifically to target the enzyme that catalyzes this reaction. Moreover, Ret-NH_2 achieved retinoid cycle slowing by selectively inhibiting the key, rate-limiting enzyme of this pathway. Lack of redundancy in its inhibitory action might significantly contribute to the high potency and lack of toxicity exhibited by Ret-NH_2.

Acknowledgment—We thank Dr. Leslie T. Webster, Jr., for valuable comments on the manuscript.

REFERENCES

1. Palczewski, K. (2006) *Annu. Rev. Biochem.* **75,** 743–767
2. Travis, G. H., Golczak, M., Moise, A. R., and Palczewski, K. (2007) *Annu. Rev. Pharmacol. Toxicol.* **47,** 469–512
3. McBee, J. K., Palczewski, K., Baehr, W., and Pepperberg, D. R. (2001) *Prog. Retin. Eye Res.* **20,** 469–529
4. Lamb, T. D., and Pugh, E. N., Jr. (2004) *Prog. Retin. Eye. Res.* **23,** 307–380
5. Jin, M., Li, S., Moghrabi, W. N., Sun, H., and Travis, G. H. (2005) *Cell* **122,** 449–459
6. Moiseyev, G., Chen, Y., Takahashi, Y., Wu, B. X., and Ma, J. X. (2005) *Proc. Natl. Acad. Sci. U. S. A.* **102,** 12413–12418
7. Redmond, T. M., Poliakov, E., Yu, S., Tsai, J. Y., Lu, Z., and Gentleman, S. (2005) *Proc. Natl. Acad. Sci. U. S. A.* **102,** 13658–13663
8. Acland, G. M., Aguirre, G. D., Ray, J., Zhang, Q., Aleman, T. S., Cideciyan, A. V., Pearce-Kelling, S. E., Anand, V., Zeng, Y., Maguire, A. M., Jacobson, S. G., Hauswirth, W. W., and Bennett, J. (2001) *Nat. Genet.* **28,** 92–95
9. Acland, G. M., Aguirre, G. D., Bennett, J., Aleman, T. S., Cideciyan, A. V., Bennicelli, J., Dejneka, N. S., Pearce-Kelling, S. E., Maguire, A. M., Palczewski, K., Hauswirth, W. W., and Jacobson, S. G. (2005) *Mol. Ther.* **12,** 1072–1082
10. Jacobson, S. G., Acland, G. M., Aguirre, G. D., Aleman, T. S., Schwartz, S. B., Cideciyan, A. V., Zeiss, C. J., Komaromy, A. M., Kaushal, S., Roman, A. J., Windsor, E. A., Sumaroka, A., Pearce-Kelling, S. E., Conlon, T. J., Chiodo, V. A., Boye, S. L., Flotte, T. R., Maguire, A. M., Bennett, J., and Hauswirth, W. W. (2006) *Mol. Ther.* **13,** 1074–1084
11. Aleman, T. S., Jacobson, S. G., Chico, J. D., Scott, M. L., Cheung, A. Y., Windsor, E. A., Furushima, M., Redmond, T. M., Bennett, J., Palczewski, K., and Cideciyan, A. V. (2004) *Invest. Ophthalmol. Vis. Sci.* **45,** 1259–1271
12. Jacobson, S. G., Aleman, T. S., Cideciyan, A. V., Heon, E., Golczak, M., Beltran, W. A., Sumaroka, A., Schwartz, S. B., Roman, A. J., Windsor, E. A., Wilson, J. M., Aguirre, G. D., Stone, E. M., and Palczewski, K. (2007) *Proc. Natl. Acad. Sci. U. S. A.* **104,** 15123–15128
13. Batten, M. L., Imanishi, Y., Tu, D. C., Doan, T., Zhu, L., Pang, J., Glushakova, L., Moise, A. R., Baehr, W., Van Gelder, R. N., Hauswirth, W. W., Rieke, F., and Palczewski, K. (2005) *PLoS Med.* **2,** 1177–1189
14. Van Hooser, J. P., Aleman, T. S., He, Y. G., Cideciyan, A. V., Kuksa, V., Pittler, S. J., Stone, E. M., Jacobson, S. G., and Palczewski, K. (2000) *Proc. Natl. Acad. Sci. U. S. A.* **97,** 8623–8628
15. Van Hooser, J. P., Liang, Y., Maeda, T., Kuksa, V., Jang, G. F., He, Y. G., Rieke, F., Fong, H. K., Detwiler, P. B., and Palczewski, K. (2002) *J. Biol. Chem.* **277,** 19173–19182
16. Rohrer, B., Goletz, P., Znoiko, S., Ablonczy, Z., Ma, J. X., Redmond, T. M., and Crouch, R. K. (2003) *Invest. Ophthalmol. Vis. Sci.* **44,** 310–315
17. Radu, R. A., Mata, N. L., Nusinowitz, S., Liu, X., Sieving, P. A., and Travis, G. H. (2003) *Proc. Natl. Acad. Sci. U. S. A.* **100,** 4742–4747
18. Radu, R. A., Han, Y., Bui, T. V., Nusinowitz, S., Bok, D., Lichter, J., Widder, K., Travis, G. H., and Mata, N. L. (2005) *Invest. Ophthalmol. Vis. Sci.* **46,** 4393–4401
19. Radu, R. A., Mata, N. L., Bagla, A., and Travis, G. H. (2004) *Proc. Natl. Acad. Sci. U. S. A.* **101,** 5928–5933
20. Radu, R. A., Mata, N. L., Nusinowitz, S., Liu, X., and Travis, G. H. (2004) *Novartis Found. Symp.* **255,** 51–63; discussion 63–67, 177–178
21. Finnemann, S. C., Leung, L. W., and Rodriguez-Boulan, E. (2002) *Proc. Natl. Acad. Sci. U. S. A.* **99,** 3842–3847
22. De, S., and Sakmar, T. P. (2002) *J. Gen. Physiol.* **120,** 147–157
23. Bergmann, M., Schutt, F., Holz, F. G., and Kopitz, J. (2004) *FASEB J.* **18,** 562–564
24. Conley, B., O'Shaughnessy, J., Prindiville, S., Lawrence, J., Chow, C., Jones, E., Merino, M. J., Kaiser-Kupfer, M. I., Caruso, R. C., Podgor, M., Goldspiel, B., Venzon, D., Danforth, D., Wu, S., Noone, M., Goldstein, J., Cowan, K. H., and Zujewski, J. (2000) *J. Clin. Oncol.* **18,** 275–283
25. Caffery, B. E., and Josephson, J. E. (1988) *J. Am. Optom. Assoc.* **59,** 221–224
26. Caruso, R. C., Zujewski, J., Iwata, F., Podgor, M. J., Conley, B. A., Ayres, L. M., and Kaiser-Kupfer, M. I. (1998) *Arch. Ophthalmol.* **116,** 759–763
27. Gamble, M. V., Mata, N. L., Tsin, A. T., Mertz, J. R., and Blaner, W. S. (2000) *Biochim. Biophys. Acta* **1476,** 3–8
28. Gollapalli, D. R., and Rando, R. R. (2004) *Proc. Natl. Acad. Sci. U. S. A.* **101,** 10030–10035
29. Golczak, M., Kuksa, V., Maeda, T., Moise, A. R., and Palczewski, K. (2005) *Proc. Natl. Acad. Sci. U. S. A.* **102,** 8162–8167
30. Golczak, M., Imanishi, Y., Kuksa, V., Maeda, T., Kubota, R., and Palczewski, K. (2005) *J. Biol. Chem.* **280,** 42263–42273
31. Imanishi, Y., Gerke, V., and Palczewski, K. (2004) *J. Cell Biol.* **166,** 447–453
32. Imanishi, Y., Batten, M. L., Piston, D. W., Baehr, W., and Palczewski, K. (2004) *J. Cell Biol.* **164,** 373–383
33. Maiti, P., Kong, J., Kim, S. R., Sparrow, J. R., Allikmets, R., and Rando, R. R. (2006) *Biochemistry* **45,** 852–860
34. Maiti, P., Kong, J., Kim, S., Sparrow, J., Allikmets, R., and Rando, R. (2007) *Biochemistry* **46,** 8700
35. Quadro, L., Blaner, W. S., Salchow, D. J., Vogel, S., Piantedosi, R., Gouras, P., Freeman, S., Cosma, M. P., Colantuoni, V., and Gottesman, M. E. (1999) *EMBO J.* **18,** 4633–4644
36. Quadro, L., Hamberger, L., Gottesman, M. E., Wang, F., Colantuoni, V., Blaner, W. S., and Mendelsohn, C. L. (2005) *Endocrinology* **146,** 4479–4490
37. Saari, J. C., and Bredberg, D. L. (1990) *Methods Enzymol.* **190,** 156–163
38. Jones, T. H., Clark, D. A., Heterick, B. E., and Snelling, R. R. (2003) *J. Nat. Prod.* **66,** 325–326
39. Kitamura, T., Koshino, Y., Shibata, F., Oki, T., Nakajima, H., Nosaka, T., and Kumagai, H. (2003) *Exp. Hematol.* **31,** 1007–1014
40. Palczewski, K., Jager, S., Buczylko, J., Crouch, R. K., Bredberg, D. L., Hofmann, K. P., Asson-Batres, M. A., and Saari, J. C. (1994) *Biochemistry* **33,** 13741–13750
41. Stecher, H., Gelb, M. H., Saari, J. C., and Palczewski, K. (1999) *J. Biol. Chem.* **274,** 8577–8585
42. Stecher, H., and Palczewski, K. (2000) *Methods Enzymol.* **316,** 330–344
43. Kapust, R. B., Tozser, J., Fox, J. D., Anderson, D. E., Cherry, S., Copeland, T. D., and Waugh, D. S. (2001) *Protein Eng.* **14,** 993–1000
44. Maeda, A., Maeda, T., Imanishi, Y., Kuksa, V., Alekseev, A., Bronson, J. D., Zhang, H., Zhu, L., Sun, W., Saperstein, D. A., Rieke, F., Baehr, W., and Palczewski, K. (2005) *J. Biol. Chem.* **280,** 18822–18832

45. Xie, Y., Lashuel, H. A., Miroy, G. J., Dikler, S., and Kelly, J. W. (1998) *Protein Expression Purif.* **14,** 31–37
46. Cogan, U., Kopelman, M., Mokady, S., and Shinitzky, M. (1976) *Eur. J. Biochem.* **65,** 71–78
47. Maeda, A., Maeda, T., Golczak, M., Imanishi, Y., Leahy, P., Kubota, R., and Palczewski, K. (2006) *Mol. Pharmacol.* **70,** 1220–1229
48. Maeda, A., Maeda, T., Imanishi, Y., Sun, W., Jastrzebska, B., Hatala, D. A., Winkens, H. J., Hofmann, K. P., Janssen, J. J., Baehr, W., Driessen, C. A., and Palczewski, K. (2006) *J. Biol. Chem.* **281,** 37697–37704
49. Kuksa, V., Imanishi, Y., Batten, M., Palczewski, K., and Moise, A. R. (2003) *Vision Res.* **43,** 2959–2981
50. Law, W. C., and Rando, R. R. (1989) *Biochem. Biophys. Res. Commun.* **161,** 825–829
51. Kothapalli, R., Guthrie, N., Chambers, A. F., and Carroll, K. K. (1993) *Lipids* **28,** 969–973
52. Ura, H., Obara, T., Shudo, R., Itoh, A., Tanno, S., Fujii, T., Nishino, N., and Kohgo, Y. (1998) *Mol. Carcinog.* **21,** 93–99
53. Khalil, A. A., Steyn, S., and Castagnoli, N., Jr. (2000) *Chem. Res. Toxicol.* **13,** 31–35
54. Edmondson, D. E., Binda, C., and Mattevi, A. (2007) *Arch. Biochem. Biophys.* **464,** 269–276
55. Kawaguchi, R., Yu, J., Honda, J., Hu, J., Whitelegge, J., Ping, P., Wiita, P., Bok, D., and Sun, H. (2007) *Science* **315,** 820–825
56. Batten, M. L., Imanishi, Y., Maeda, T., Tu, D. C., Moise, A. R., Bronson, D., Possin, D., Van Gelder, R. N., Baehr, W., and Palczewski, K. (2004) *J. Biol. Chem.* **279,** 10422–10432
57. De Laey, J. J., and Verougstraete, C. (1995) *Retina* **15,** 399–406
58. Wabbels, B., Demmler, A., Paunescu, K., Wegscheider, E., Preising, M. N., and Lorenz, B. (2006) *Graefes Arch. Clin. Exp. Ophthalmol.* **244,** 36–45
59. Suter, M., Reme, C., Grimm, C., Wenzel, A., Jaattela, M., Esser, P., Kociok, N., Leist, M., and Richter, C. (2000) *J. Biol. Chem.* **275,** 39625–39630
60. Eldred, G. E. (1993) *Nature* **364,** 396
61. Schutt, F., Davies, S., Kopitz, J., Holz, F. G., and Boulton, M. E. (2000) *Invest. Ophthalmol. Vis. Sci.* **41,** 2303–2308
62. Sparrow, J. R., Nakanishi, K., and Parish, C. A. (2000) *Invest. Ophthalmol. Vis. Sci.* **41,** 1981–1989
63. Steinberg, R. H. (1985) *Doc. Ophthalmol.* **60,** 327–346
64. Mata, N. L., Weng, J., and Travis, G. H. (2000) *Proc. Natl. Acad. Sci. U. S. A.* **97,** 7154–7159
65. Maiti, P., Gollapalli, D., and Rando, R. R. (2005) *Biochemistry* **44,** 14463–14469
66. Fujii, H., Sato, T., Kaneko, S., Gotoh, O., Fujii-Kuriyama, Y., Osawa, K., Kato, S., and Hamada, H. (1997) *EMBO J.* **16,** 4163–4173
67. Muindi, J. R., Young, C. W., and Warrell, R. P., Jr. (1994) *Leukemia* **8,** Suppl. 3, 16–21
68. Berni, R., and Formelli, F. (1992) *FEBS Lett.* **308,** 43–45
69. Vogel, S., Piantedosi, R., O'Byrne, S. M., Kako, Y., Quadro, L., Gottesman, M. E., Goldberg, I. J., and Blaner, W. S. (2002) *Biochemistry* **41,** 15360–15368
70. Blaner, W. S., Hendriks, H. F., Brouwer, A., de Leeuw, A. M., Knook, D. L., and Goodman, D. S. (1985) *J. Lipid Res.* **26,** 1241–1251
71. Noy, N., and Xu, Z. J. (1990) *Biochemistry* **29,** 3888–3892
72. McBee, J. K., Van Hooser, J. P., Jang, G. F., and Palczewski, K. (2001) *J. Biol. Chem.* **276,** 48483–48493
73. Sagami, H., Korenaga, T., Ogura, K., Steiger, A., Pyun, H. J., and Coates, R. M. (1992) *Arch. Biochem. Biophys.* **297,** 314–320
74. Dolence, J. M., and Poulter, C. D. (1995) *Proc. Natl. Acad. Sci. U. S. A.* **92,** 5008–5011
75. Huang, C., Hightower, K. E., and Fierke, C. A. (2000) *Biochemistry* **39,** 2593–2602
76. Coxon, F. P., Helfrich, M. H., Larijani, B., Muzylak, M., Dunford, J. E., Marshall, D., McKinnon, A. D., Nesbitt, S. A., Horton, M. A., Seabra, M. C., Ebetino, F. H., and Rogers, M. J. (2001) *J. Biol. Chem.* **276,** 48213–48222
77. Molnar, G., Dagher, M. C., Geiszt, M., Settleman, J., and Ligeti, E. (2001) *Biochemistry* **40,** 10542–10549
78. Isken, A., Holzschuh, J., Lampert, J. M., Fischer, L., Oberhauser, V., Palczewski, K., and von Lintig, J. (2007) *J. Biol. Chem.* **282,** 1144–1151
79. Canada, F. J., Law, W. C., Rando, R. R., Yamamoto, T., Derguini, F., and Nakanishi, K. (1990) *Biochemistry* **29,** 9690–9697